WWW.IJRPR.COM

International Journal of Research Publication and Reviews

Journal homepage: www.ijrpr.com ISSN 2582-7421

THERAPEUTIC POTENTIAL OF NASAL TRANS-FERULIC ACID NANOEMULSION FOR ALZHEIMER'S DISEASE

Rupesh Kumar Gupta[1] , Dr Rakesh Kumar Gawaly [2] , Dr Kavita R. Loksh[3]

[1] Research Scholar,Oriental College of Pharmacy, Bhopal, M.P.
[2] Professor, Oriental College of Pharmacy, Bhopal, M.P.
[3] Director, Oriental College of Pharmacy, Bhopal, M.P.

ABSTRACT :

This study explores the formulation of a trans-ferulic acid-loaded nanoemulsion (TFA-NE) as a novel approach for treating Alzheimer's disease (AD). Trans-ferulic acid, a natural compound with neuroprotective and antioxidant properties, suffers from low bioavailability due to its BCS Class II classification. The nanoemulsion, composed of lavender oil, Tween 80, and PEG 200, enhances the solubility and stability of trans-ferulic acid. Characterization studies confirmed its optimal particle size (125.9–152.6 nm), zeta potential (-7.39 mV), and spherical morphology. In-vitro studies demonstrated improved drug release (85.40% over 14 hours at pH 6.3), antioxidant activity (71.21%), and acetylcholinesterase inhibition (48.14%). Stability tests indicated the formulation's robustness under refrigerated conditions for three months. These findings suggest that TFA-NE provides a promising therapeutic strategy for AD by facilitating targeted drug delivery and enhancing bioavailability.

Keywords Trans-ferulic acid Nanoemulsion Alzheimer's disease Bioavailability, Nasal drug

Introduction :

Alzheimer's disease (AD) is a progressive neurological disorder characterized by the death and loss of function of nerve cells in various brain regions. Alzheimer's disease damages neuronal cells that produce and use acetylcholine. Globally, over 50 million people have dementia. It is the most prevalent type of dementia (1). It usually starts in late middle age or old age (above 65 years). In the year 2019, the certified death rate progress was reported to be 121,499 owing to AD. The irreversible neurodegenerative illness known as Alzheimer's disease (AD), which causes a decrease in memory and executive function as well as personality changes, affects around two- thirds of people(2). It is described as Alois Alzheimer's name, who in 1906 first described AD. Synapse loss and neuronal shrinkage are the main outcomes of AD in the cerebral cortex and hippocampal regions. Neurofibrillary tangles (NFTs) and β-amyloid (Aβ) plaques are the two main pathologies of Alzheimer's diseaseSigns and symptoms

- memory loss,
- language problems
- mood swings,
- personality changes
- wandering
- agitation
- confusion
- motor disturbances
- unable to perform

Treatment of Alzheimer's disease

The US FDA-approved treatment options or therapeutics available are donepezil, rivastigmine, tacrine, galantamine, and memantine. The currently US FDA-approved treatments for Alzheimer's disease include memantine, an NMDA (N-methyl-D-aspatarte)-receptor antagonist, for moderate to severe Alzheimer's dementia, and acetylcholinesterase (AchE) inhibitors for mild to moderate instances. Nevertheless, none of the current treatments appear to be able to treat Alzheimer's dementia or halt the disease's development (11). All of these medications appear to be able to provide some patients with moderate symptom improvements. There is a great need in medicine

for the advancement of innovative treatment approaches that aim to address the underlying pathogenic processes of Alzheimer's disease, which should result in the development of new drugs with potent disease-modifying abilities (12).

Nanoemulsion (as a Nono-carrier)

A biphasic liquid dose form is called a nanoemulsion. Nanoemulsion is a transparent, clear liquid dosage form for the targeted drug delivery system. The droplet size of the nanoemulsion ranges from 20-100 nm, and the droplet size is less than that of microemulsions; they look cleaner or hazier. It is made up of two immiscible liquid phases: one is a liquid phase, and the other is an oil phase. One phase is called the dispersed phase, and another is the continuous phase(13). An amphiphilic surfactant like soy lecithin, span tween, etc stabilizes nanoemulsion. Nanoemulsion may have different types depending on both phases, such as water in oil (W/O) or oil in water (O/W) droplets. Because of their intrinsic energy, nanoemulsions are thermodynamically unstable liquid doses

Advantages of nanoemulsion

- Increased bioavailability of the drugs
- Provide release of the drug at the target site
- Provide prolonged release of the drugs
- Low energy is required.
- Cost-effective
- Increased solubility of the drugs.
- Non-toxic and non-irritant in nature
- Nanoemulsions can be easily converted into gel form(16)

Disadvantages of nanoemulsion

- Thermodynamically unstable system.
- A large amount of surfactant and co-surfactant is required for stabilization.
- Limited use for high melting point drug substances(17).

Characterization of Nanoemulsions

Different types of techniques and methods are used for the characterization of the nanoemulsions, which are described below;

Particle Size and Size Distribution Dynamic Light Scattering (DLS):

- Measures the size distribution of nanoparticles based on their Brownian motion.
- Provides information on the mean particle size and polydispersity index (PDI), indicating size uniformity.

Transmission Electron Microscopy (TEM) and Scanning Electron Microscopy (SEM):

- Provides visual confirmation of particle size and morphology.
- TEM offers high-resolution images, while SEM provides surface topography.

Photon Correlation Spectroscopy (PCS):

- Similar to DLS, used for measuring the particle size distribution in colloidal dispersions.

Zeta Potential

Electrophoretic Light Scattering (ELS):

- Measures the zeta potential, which indicates the surface charge of nanoemulsions.
- Important for assessing the stability of nanoemulsions; higher zeta potential values generally indicate better stability due to electrostatic repulsion between particles.

Surface Morphology and Structure Atomic Force Microscopy (AFM):

- Provides detailed topographical images of nanoemulsions at the nanometer scale.
- Useful for studying surface roughness and particle interactions.

Encapsulation Efficiency and Drug Loading Ultracentrifugation:

- Separates the free drug from the encapsulated drug.
- Measurement of drug concentration in the supernatant and pellet helps calculate encapsulation efficiency and drug loading capacity.

High-Performance Liquid Chromatography (HPLC):

- Quantifies the amount of drug encapsulated within the nanoemulsions.
- Determines encapsulation efficiency and drug loading.

Stability Studies Thermodynamic Stability Tests:

- Involves heating-cooling cycles, centrifugation, and freeze-thaw cycles to test the physical stability of nanoemulsions.

Accelerated Stability Testing:

- Uses elevated temperatures and humidity to predict the long-term stability of nanoemulsions.

Visual Inspection:

- Regular observation for signs of phase separation, creaming, or sedimentation.

Rheological Properties Viscosity Measurement:

- Determines the flow behavior and viscosity of nanoemulsions using rheometers.
- Important for understanding the ease of administration and spreading properties.

Phase Behavior

Phase Diagram Construction:

- Helps understand nanoemulsions' phase behavior at different temperatures and compositions.
- Important for identifying the optimal formulation conditions.

Interfacial Tension Pendant Drop Method:

- Measures the interfacial tension between the oil and water phases.
- It is crucial for understanding the emulsification process and stability.

Thermal Analysis

Differential Scanning Calorimetry (DSC):

- Measures the thermal properties of nanoemulsions.
- Useful for studying the phase transition temperatures and thermal stability.

Thermogravimetric Analysis (TGA):

- Determines the weight loss as a function of temperature.
- Provides information on the thermal stability and composition.

Spectroscopic Techniques

Fourier Transform Infrared Spectroscopy (FTIR):

- Analyzes the chemical composition and functional groups of the components in nanoemulsions.
- Helps in confirming the encapsulation of drugs and the interaction between components.

Nuclear Magnetic Resonance (NMR):

- Provides detailed information on the molecular structure and dynamics of the nanoemulsion components.
- Useful for studying the interaction between the drug and the emulsifying agents.

pH Measurement

pH Meter:

- Monitors the pH of nanoemulsions, which can influence stability and drug release profiles.

Drug Release Kinetics Dialysis Method:

- Helps in understanding the release mechanism and rate of drug delivery.

***In-Vitro* Release Studies:**

- Uses simulated biological fluids to study the drug release kinetics.
- Provides information on the release rate and pattern of the encapsulated drug(48)

Materials and methods :

Materials

Materials	Supplier
Tras-ferulic acid (TFA)	Yarrow Pharma Pvt. Ltd
Lavender oil	Gift sample
DPPH	CDH, India
surfactants	Research lab fine chem, Islampur

n-octanol	Loba Chemical Mumbai, India
methanol	CDH, India
Dialysis bag	CDH, India

Methods

Preformulation Studies of Trans-ferulic Acid (TFA)

Research initiatives focused on preformulation can potentially advance the identification of new active components or define the physical properties needed to create dosage forms. Important information supplied during the formulation process can help ensure the effective and prompt launch of novel pharmaceutical substances for human use. Pre-formulation studies are essential for characterizing medications to properly design drug delivery systems. The formulation seeks to determine the molecular and physical properties that will contribute to developing a stable, secure, and efficient formulation with the highest bioavailability(58).

Physical appearance

The TFA was observed visually, and the results showed a very fine white powder. Trans-ferulic Acid fine particle and crystalline characteristics were determined by microscopic evaluation using an optical microscope.

Melting Point Determination

The capillary melting technique was used to determine the trans-ferulic acid melting point. This technique involves filling the capillary with a tiny amount of medication and storing it within the digital melting (Jyoti Scientific Industry, Gwalior M.P.). Afterward, the analysis will begin to show the trans-ferulic acid melting point on the instrument's viewable screen for recording.

Identification of Drug

Trans-ferulic Acid was identified using a UV-visible spectrophotometer, infrared spectroscopy, melting point determination, and solubility study.

Identification of drug by UV-Visible spectrophotometer

UV-visible spectroscopy determined the wavelength at which trans-ferulic acid shows maximum absorbance. Furthermore, 5 mg of trans-ferulic acid was dissolved in 10 ml of methanol. The sample was scanned between the 800-200 nm range using a UV-visible spectrophotometer (Carry Win-60, UV-visible spectrophotometer, Agilent, USA)(59).

Identification of Drug by Fourier Transmittance Infra-red spectroscopy (FTIR)

A Fourier Transmittance Infra-red spectroscopy (Model Perkin Elmer, USA) was used to identify and evaluate trans-ferulic acid. The potassium bromide (KBr) pellet method was employed in this experiment. The materials were thoroughly combined with dry powdered KBr crystals. Compressing the mixture produced a disk. The disc was examined using a spectrophotometer, and its spectra were noted.

Identification of Drug by X-ray Diffraction

The X-ray diffraction pattern of pure trans-ferulic acid was examined using an X-ray diffractometer (Rigaku Smart Lab, USA). A 40 kV voltage and 30 mA current were applied to the copper anode. All samples were scanned using a scintillation counter detector with a 2Ɵ angle range of 5.010 to 50°. The change, if any, in the unique XRD peak was investigated using previously published data.

2.3.7 Identification of Drug by Differential Scanning Calorimetry (DSC)

A differential scanning calorimeter (DSC) is a thermoanalytical technique that measures the difference in heat required to raise the temperature of a sample and a reference as a function of temperature. The reference and sample were discussed during the experiment at temperatures similar to the sample temperature(60).

2.3.8 Partition Coefficient

The drug's partition coefficient was determined by dissolving 10 mg of trans-ferulic acid to equilibrate in a combination of n-octanol/water comprising 10 mL of each, swirling the mixture on a vortex mechanical shaker for 24 hours, and then keeping it in a separating funnel overnight at 37±2°C. Following the separation of the two layers, the drug concentration in each layer was measured at 310 nm by using a UV spectrophotometer (Shimadzu UV-1700 series) . The partition coefficient was then calculated using the following method(61).

PO/w = Concentration of drug in n-octanol /Concentration of drug in water

2.3.8 Solubility Study

The drug's solubility was examined in various solvents, such as distilled water, acetone, methanol, DMSO, and ethanol. A predetermined amount of medication was added to several volumetric flasks with different solvents. After adding too much of the medication to different solvents until the solution became saturated, the volumetric flask was shaken continuously for 24 hours at a steady temperature (25^0C) using a mechanical shaker (Jyoti Scientific and Industry, Gwalior). After the saturated solution was ready, it was diluted, filtered, and examined using a UV spectrophotometer. Before every sample, three calculations were made to determine how soluble trans-ferulic acid was in various solvents.

Preparation of Calibration curve of trans-ferulic acid in PBS (pH 6.3)

A trans-ferulic acid calibration curve was prepared by dissolving 10 mg of trans-ferulic acid in 10 ml of PBS (pH 6.3) from stock solution 100 (µg/ml) serial dilution was done (2, 4, 6, 8, 10, & 12 µg/ml) by scanning the solution in a UV-Visible spectrophotometer (Carry Win-60, UV-Visible Spectrophotometer, Agilent, USA) at 310 nm.

Preparation of Calibration Curve trans-ferulic acid in water

A trans-ferulic acid calibration curve was prepared by dissolving 10 mg of trans-ferulic acid in 10 ml of water from stock solution 100 (µg/ml) serial dilution was done (2, 4, 6, 8, 10, & 12 µg/ml) by scanning the solution in a UV-Visible spectrophotometer (Carry Win-60, UV-Visible Spectrophotometer, Agilent, USA) at 310 nm.

2.6 Compatibility Study

A physical mixture of trans-ferulic acid and excipients was analyzed using FTIR (4000-400 cm^{-1}).

2.7 Nanoemulsion Components

Solubility was tested in oils (labrafil M, lavender oil, oleic oil), surfactants (Cremophore RH40, Tween 80, Span 20), and co-surfactants (PEG 400, PEG 200, PEG 600, Span 80). Lavender oil, Tween 80, and PEG 200 were selected.

2.8 Pseudoternary Phase Diagram

A phase diagram was created using MODDE software (oil: 10-50%, surfactant: 30-40%, co-surfactant: 20-30%) to identify optimal formulations.

2.9 Preparation of Nanoemulsions

Nanoemulsions using lavender oil, Tween 80, and PEG 200 were sonicated (20 kHz, 5 min, 37°C). TFA was added and vortexed for solubilization.

2.9.1 Characterization of of Nanoemulsions-

2.9.1.1 Particle Size, PDI, and Zeta Potential

Zeta Sizer was used to measure particle size, PDI, and zeta potential at 25°C.

2.10 Surface Morphology

TEM and SEM analyzed morphology using carbon-coated copper grids stained with phosphotungstic acid.

2.11 Drug Content

10 µL of TFA nanoemulsion was diluted with methanol and analyzed by UV-Vis spectrophotometry. Drug content (%) = (Dissolved drug / Added drug) × 100.

2.12 In-vitro Drug Release

Drug release using a dialysis membrane in PBS (pH 6.3) at 37°C was measured at 310 nm. Kinetics were modeled with zero-order, first-order, Higuchi, Hixson-Crowell, and Korsmeyer-Peppas models.

2.13 Stability Study

Stability was evaluated by centrifugation (10,000 rpm, 30 min) and storage at 3±5°C and 40±2°C/75±5% RH for 3 months.

2.14 Antioxidant Activity

DPPH radical scavenging activity was measured at 517 nm. Radical scavenging (%) = [(Abs control - Abs sample) / Abs control] × 100.

2.15 Cell Viability (MTT Assay)

SH-SY5Y cells treated with TFA nanoemulsion and free TFA were assessed using MTT reagent. Viability (%) = (Abs sample / Abs control) × 100.

2.16 AChE Inhibitory Activity

AChE inhibition was tested using acetylthiocholine iodide with absorbance at 405 nm. Inhibition (%) = [1 - (Abs sample / Abs blank)] × 100.Results and discussion

Pre-formulation studies

Prior to formulation, research was done on the drug and polymer to confirm its identification, purity, and lack of significant barriers to the drug's formulation with the specified polymer and excipients. In addition to confirming the product's identity and purity, analyses revealed no proof of a significant drug-polymer interaction.

Physiochemical characterization of the drug

Organoleptic Property: The drug sample under investigation had a whitish, delicate powder appearance and no odor, similar to what was written about in the literature.

Table 3.1. Representation physicochemical properties

S. No	Characteristics	Observation
1	Appearance	Crystalline powder
2	Color	whitish
3	Odor	Odorless
4	Taste	Bitter

Melting Point

The capillary method determined the drug's melting point, 174±2ºC, as published values (172 to 180°C). The pre-formulation study describes the melting point.

Table 3.2. Representation of the melting point of trans-ferulic acid

Reported value	Observe value
172-180^{0}C	174±2^{0}C

All data are expressed as (Mean±SD)

Identification of Drug by UV-visible spectroscopy

UV-visible spectroscopy determined the wavelength at which trans-ferulic acid shows maximum absorbance. The absorption maxima (λmax) of trans-ferulic acid were found to be 310 nm in methanol by UV- Visible Spectrophotometer (Carry Win-60, UV-visible Spectrophotometer, Agilent, USA) as shown in Fig below. 3.1(67).

Figure 3.1. Representation absorption maxima (λmax) of trans-ferulic acid

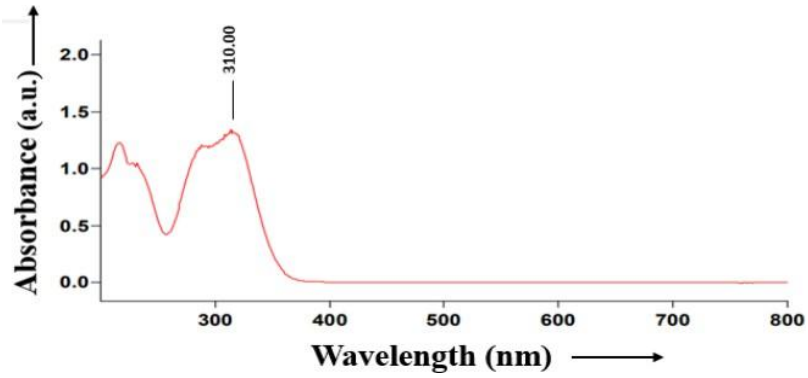

Identification of Drug by Infrared Spectroscopy FTIR

The FTIR spectrum of the trans-ferulic acid was measured by KBr using an FTIR spectrophotometer (Model Perkin Elmer, USA). The principal drug peaks were identified and compared to the drug's standard FTIR, confirming the drug's identity and purity.

In the FTIR spectrum of TFA, peaks were observed at 3531 cm-1, corresponding to the O-H stretching of the carboxylic group and 2961 cm-1 to the C-H stretching alkane group. Furthermore, another peak at 1665 cm^{-1} corresponds to C=O stretching, and a peak at 1280 cm-1 corresponds to the C-O stretching. However, the peak that appeared at 1080 cm-1 showed the bending of the C-

O groups, as shown in Fig. 3.2. All the corresponding peaks show the nearest values with their reported values, confirming the trans-ferulic acid identification.

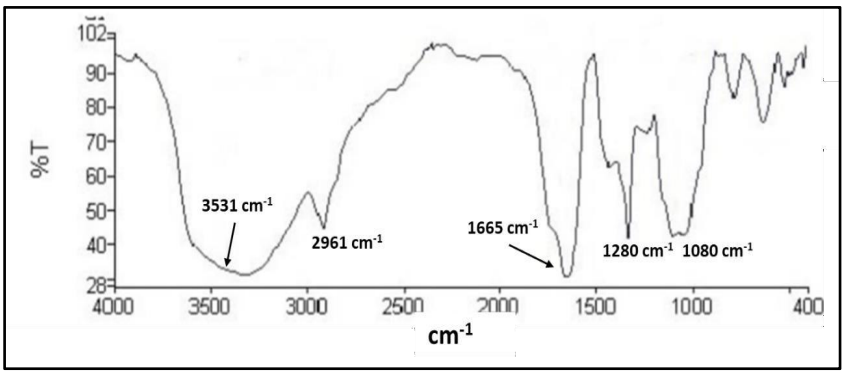

Figure 3.2. Shows the FTIR spectra of the trans-ferulic acid

Identification of Drug by X-ray diffraction

The XRD diffraction patterns for the materials are shown in Fig 3.3. The diffraction pattern of trans-ferulic acid (Drug) showed characteristic peaks at 2θ of 9.24°, 12.96°, 15.80°, 26.67°, and
29.73° indicating the crystalline nature of the drug and minor peaks at 21°, 24.5°, 31.5°, 34.6°, and 39°. Wang et al. also found a similar characteristic peak of trans-ferulic acid. The XRD pattern of trans-ferulic acid showed intense, sharp peaks that prove the crystalline nature of the compound.

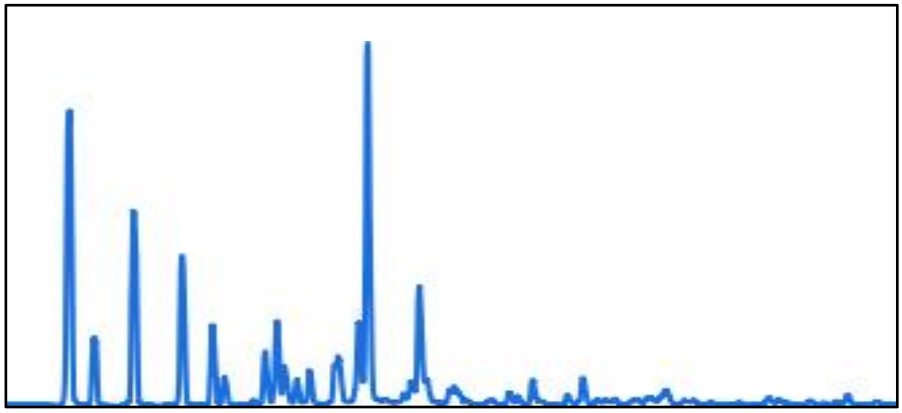

Figure 3.3. Representation of XRD spectra of the trans-ferulic acid

Identification of drug by Differential scanning calorimeter (DSC)

The drug and excipient compatibility study by DSC (TA DSC25, USA) trans-ferulic acid was shown in Fig. 3.4. The sharp endothermic peak appeared at a glass transition temperature (Tg) of 174°C, indicating the trans-ferulic acid's crystalline nature. The second broad endothermic peak shows degradation of the trans-ferulic acid(68).

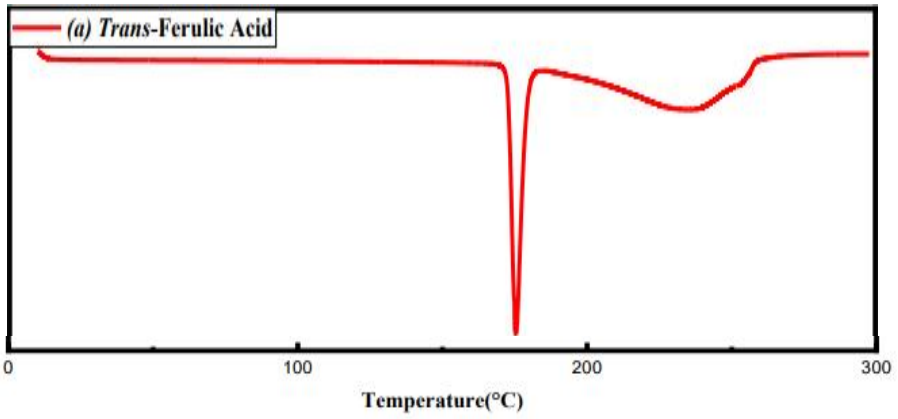

Figure 3.4. Showing the DSC spectra of the trans-ferulic acid

3.1.11 Determination of Partition Coefficient

The shake flask method determined the lipophilicity or hydrophilicity of train-ferulic acid as the partition coefficient (Log P value). Log P value for n-octanol/water was 1.501± 0.02, indicating the lipophilic nature of trans-ferulic acid.

3.1.12 Solubility study of trans-ferulic acid

The drug's solubility was investigated; it was found to be soluble in acetone (95±6 mg), sparingly soluble in methanol (70±2.3 mg), ethanol (75± 4 mg), DMSO (52±3 mg), and slightly soluble in distilled water (1± 0.05 mg). Moreover, trans-ferulic acid was more soluble in acetone than in other solvents, as shown in Fig.3.7.

Furthermore, because trans-ferulic acid is poorly soluble in aqueous solvents, the solubility data showed it is a trans-ferulic acid in the BCS-II class. The developed nanoemulsion-based formulation thereby enhances its aqueous solubility. According to Mahire and Patel (2020), trans- ferulic acid has a lower solubility in aqueous solvents like water than in other solvents.

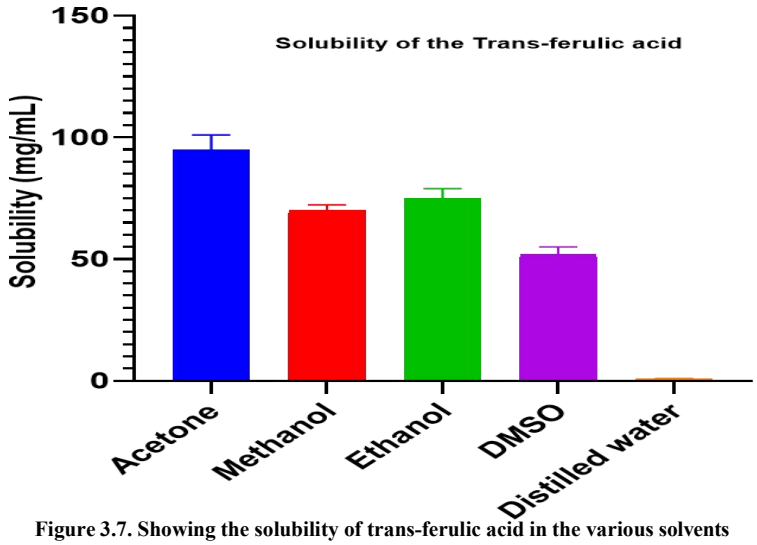

Figure 3.7. Showing the solubility of trans-ferulic acid in the various solvents

Table 3.5. Showing solubility of trans-ferulic acid in the various solvents

S. No	Components	Solubility (mg/mL)
1	Acetone	95±6
2	Methanol	70±2.3
3	Ethanol	75±4
4	DMSO	52±3
5	Water	1±0.05

Standard Calibration Curve of trans-ferulic acid in Methanol

The calibration curve of trans-ferulic acid in ethanol was carried out using a UV Visible Spectrophotometer (Shimadzu UV -1700 series) previously described method. The absorbance results for all the prepared concentrations were plotted, i.e., Concentration vs. Absorbance. The method was found to be linear over the prepared concentration range with the standard equation y= 0.07882x + 0.01600, and the Regression value was found to be 0.9990, as shown in Fig 3.5.

Table 3.3. Showing conc. Vs. Abs value in methanol

Concentration (µg/ml)	Asorbance (Mean ± SD) (at 337 nm)
12	0.9510 ± 0.027
10	0.7934 ± 0.028
8	0.6514 ± 0.031
6	0.5012 ± 0.034
4	0.3427 ± 0.023
2	0.1764 ± 0.029

Data is represented as mean ± SD (n=3)

Figure 3.5. Representation standard calibration of Trans-ferulic acid in methanol

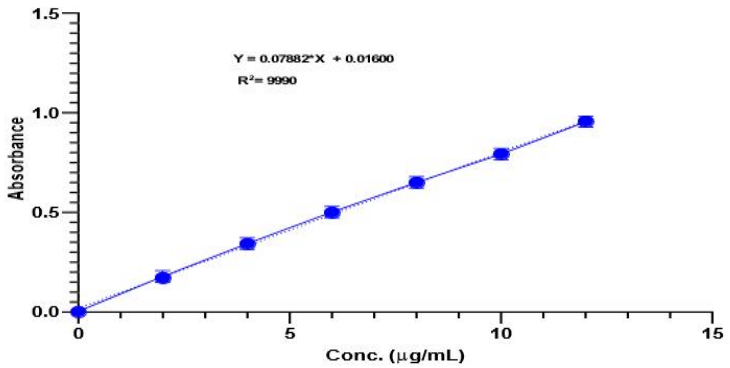

Standard Calibration Curve of trans-ferulic acid in water

The calibration curve of trans-ferulic acid in water was carried out using a UV Visible Spectrophotometer (Shimadzu UV -1700 series) previously described method. The absorbance results for all the prepared concentrations were plotted, i.e., Concentration vs. Absorbance. The method was found to be linear over the prepared concentration range with the standard equation y= 0.07703x + 0.03100, and the Regression value was found to be 0.9959, as shown in Fig.3.6(69). **Table 3.4.** Showing conc. Vs. Abs value in water

Concentration (µg/ml)	Asorbance (Mean ± SD) (at 337 nm)
12	0.9371 ± 0.027
10	0.7934 ± 0.019
8	0.6514 ± 0.031
6	0.5212 ± 0.021
4	0.3627 ± 0.023
2	0.1864 ± 0.054

Data is represented as mean ± SD (n=3)

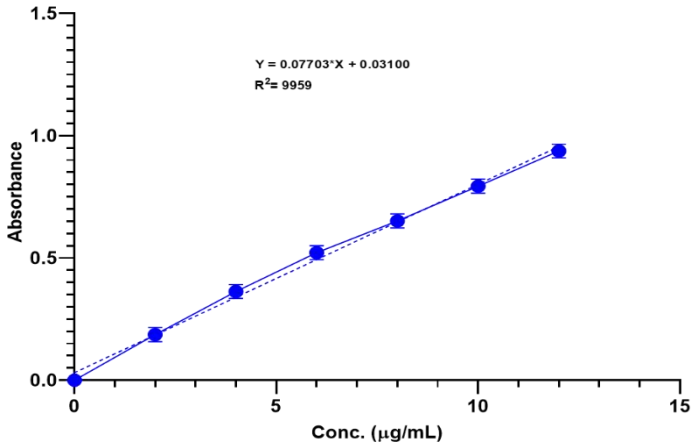

Figure 3.6. Representation standard calibration of Trans-ferulic acid in methanol

Selection of components of Nanoemulsion

Various oils like lavender, labrafil M, and oleic oil were screened for the solubility of trans-ferulic acid and its possible use as an oil phase in the NE. These essential oils are highly concentrated, aromatic oils of plant origin, having various neuroprotective activities. The oil with the highest solubility of PIP was selected as the oil phase to maximize the drug loading and minimize the amount of surfactant. Solubility of trans-ferulic acid was found to be 471.23 ± 0.97 mg/mL in lavender oil, 302.50 ± 0.108 mg/mL in labrafil M oil, and 241.46 ± 5.5 mg/mL in oleic oil (Fig. 3.8A). The results reveal that trans-ferulic acid showed the highest solubility in lavender oil compared to labrafil M and oleic oil. Further, lavender oil is also reported to have neuroprotective and cognitive enhancement effects. Solubility of trans-ferulic acid was also determined in various surfactants, including Tween 80, Span 20, and cremophor RH 40; the results are shown in Fig 3.8B. The maximum solubility of trans-ferulic acid was found to be in the 80. Tween 80 is a non- ionic surfactant that leads to the formation of o/w NE. The highest trans-ferulic acid solubility was found in PEG 200 among cosurfactants (Fig.3.8C). A cosurfactant is employed alongside a surfactant to lower interfacial tension further and enhance interface mobility. This results in greater penetration of the oil into the region and increased fluidity of the interface(70).

Figure 3.8. Representation selection of the components of nanoemulsion A) selection of oils, B) selection of surfactants, C) selection of co-surfactants

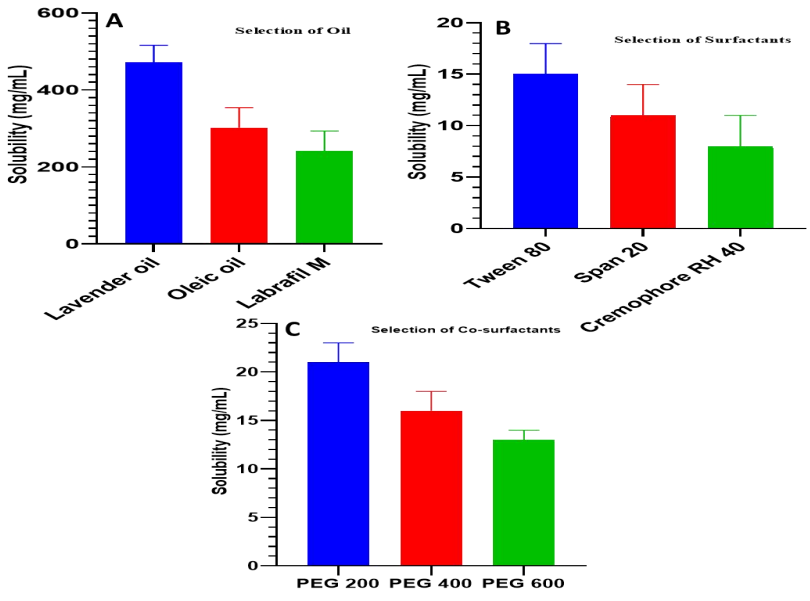

Preliminary Selection of Excipients

The solubility of the trans-ferulic acid was tested with different oils, surfactants, and co- surfactants. Finally, lavender (oil), tween 80 (surfactant), and PEG 200 (co-surfactant) were chosen for the formulation, as shown in Fig 3.8.

Compatibility Study

Fig. 3.9 (A) represents the FTIR spectra of lavender oil. The band at 3323 cm^{-1}, 2931 cm^{-1}, 1624 cm-1, and 1428 cm-1 attributed to O-H stretching, C-H stretching, N-H stretching, and C-H

bending Which are characteristics peaks of lavender oil similar to the previously reported Kento ono et at (2020). **Fig. 3.9 (B)** represents the FTIR spectra of the physical mixture; no additional peaks appeared in these spectra because TFA is compatible with oil(71).

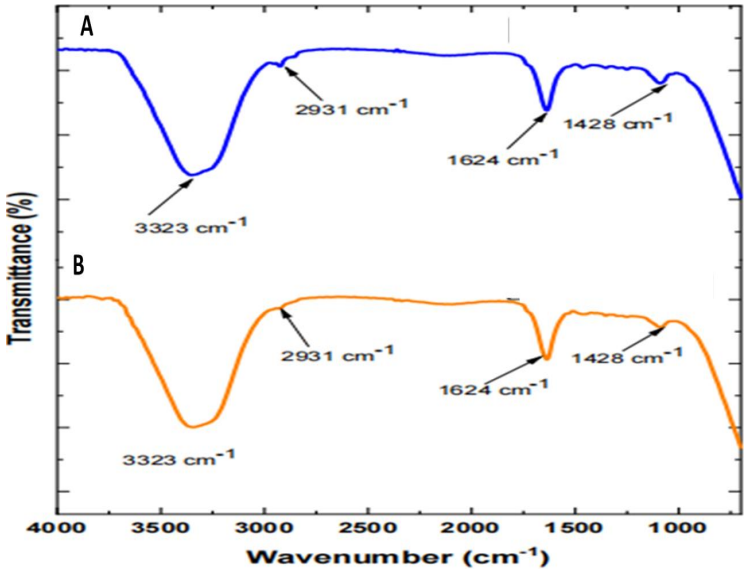

Figure 3.9. Showing FTIR spectra A) lavender oil, B) physical mixture

Construction of a Pseudo Ternary Phase Diagram

A ternary phase diagram was developed to identify the self-nano emulsifying region and the optimum concentration and combination of oil, surfactant, and co-surfactant. Ternary mixtures were prepared using excipients with a supreme transferulic acid solubilizing capacity. Percentage transmittance was selected to illustrate whether the ternary mixtures had a good or bad emulsion. Various formulations were developed and assessed for nanoemulsion physicochemical features by changing oil, surfactant, and co-surfactant concentrations. The nanoemulsion with a percentage transmittance of ≥ 85% is considered good.

Results exhibited the transparent nanoemulsion region with a purple color in the ternary phase diagram. Different concentrations of surfactants and co-surfactants were utilized in developing nanoemulsions and depicted in the ternary diagrams with varying concentrations of excipients in the ratios of 1:1, 1:2, and 2:1 shown in Fig 3.10. A–C. With varying ratios, the concentration of lavender oil was also 10–50%, while the surfactant and co-surfactant needed to be 30–40% and 20–30%, respectively.

The purple-colored area represents a crystal-clear nanoemulsion, and the yellow-colored area indicates a microemulsion. Concentrations of oil, surfactant, and co-surfactant were adjusted and optimized and are given in tab. 3.6(72)**.**

Table 3.6. Different formulation mixtures with varying concentrations of oil, surfactant, and co- surfactant.

Formulation	Surfactant to co- surfactant ratio (Km ratio)	Lavender oil (% w/w)	Tween (% w/v)	PEG 200 (% w/w)	TFA (% w/w)
1	1:1	10	44	44	1
2	1:1	20	39	39	1
3	2:1	30	45.3	22.7	1
4	2:1	49	26	23	1
5	1:2	20	26	52	1
6	1:2	0	22.7	45.3	1

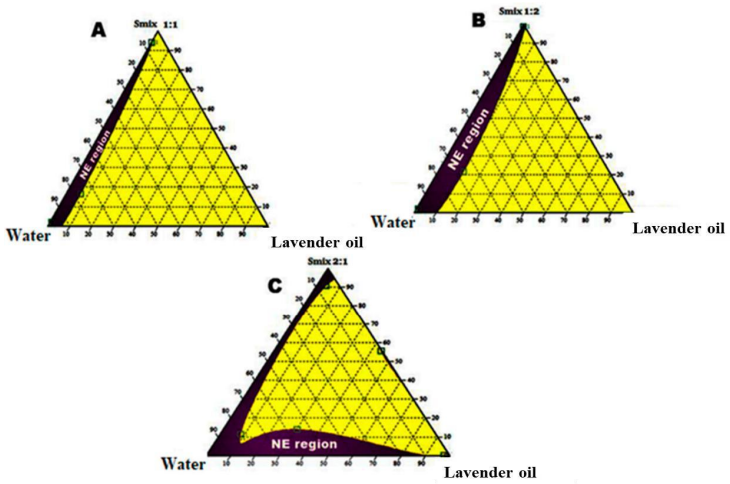

Figure 3.10. Ternary phase diagram representing the emulsification region. (A) Smix ratio = 1:1,

(B) Smix ratio = 1:2, & (C) Smix ratio = 2:1. The purple-colored area indicates nanoemulsion, and the yellow-colored area indicates microemulsion.

Particle Size, PDI, and Zeta Potential of Trans-ferulic acid loaded Nanoemulsion - Fig. 3.11. shows the average globule size of the chosen formulations, which was determined to be between 125.9 and 152.6 nm, with a polydispersity index (PDI) of 0.221 and 0.218, respectively.

The zeta potential of the blank nanoemulsion and the nanoemulsion loaded with transferulic acid

was found to be –6.95 mV and -7.39, respectively, as shown in Fig.3.11. This indicates formulation

stability since the formulation resists aggregation. Droplet size shows an inverse connection, according to the zeta potential. The optimum formulation in this case is the nanoemulsion formulation with a steady zeta potential at the nanoscale (+30 mV to -30 mV)(73).

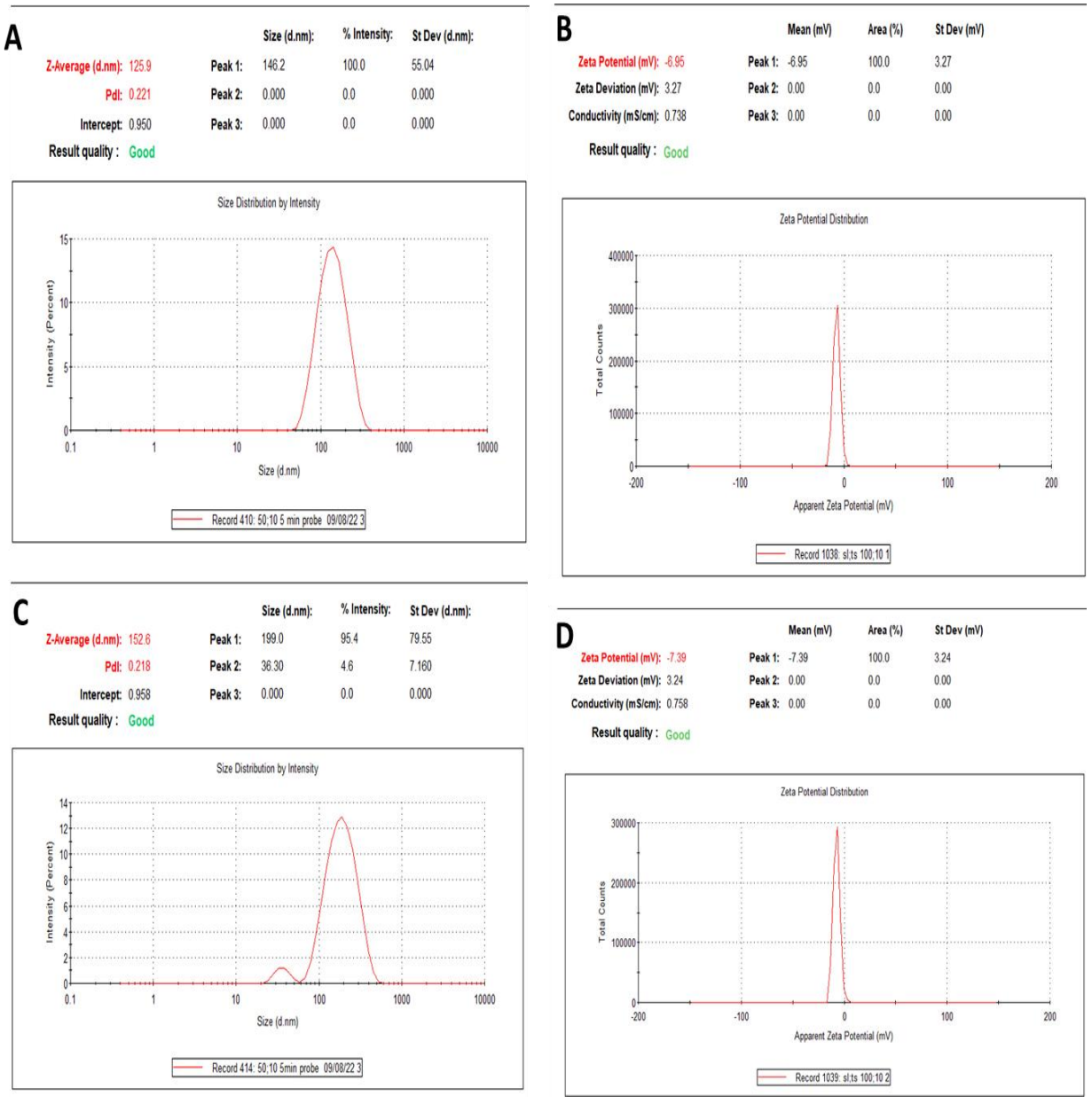

Figure 3.11. Representation globule size, PDI, and zeta potential A) Globule size of blank nanoemulsion, B) zeta potential of blank nanoemulsion, C) Globule size of trans-ferulic acid loaded nanoemulsion, D) zeta potential of trans-ferulic acid loaded nanoemulsion. Evaluation of the Surface morphology

The TEM investigation of the blank nanoemulsion in Fig. 3.12 A showed the nanoemulsion's consistent distribution and spherical shape. The variations in the principles of the two procedures create a little variation in the observed DLS results from the nanoparticles evaluated by TEM. The nanoemulsion underwent SEM investigation, revealing a spherical globule size, as shown in Fig.
3.12 B).

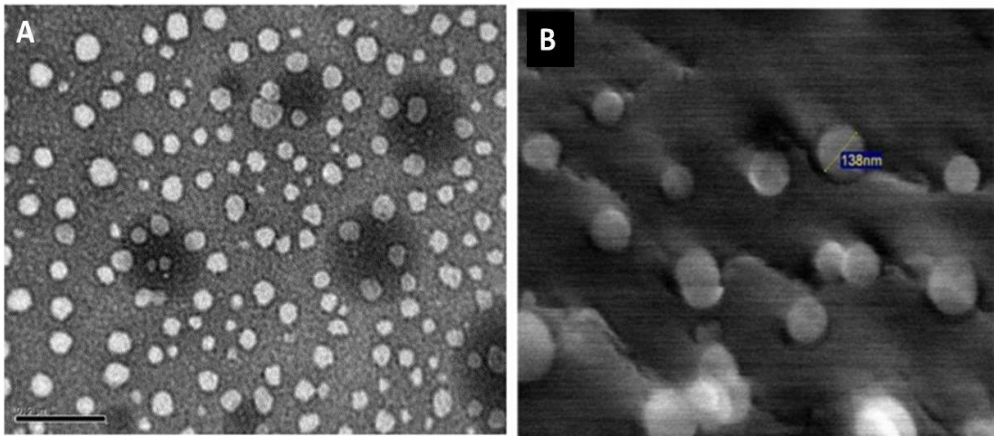

Figure 3.12. Representation morphology of B-NE A) TEM images, B) SEM

Drug entrapment efficiency

Drug entrapment efficiency was found to be 85% in trans-ferulic acid-loaded nanoemulsion. Thus, it was clear from the data that the most promising carriers for encapsulating Class II medications were manufactured TFA-based nanoemulsions.

***In-vitro* drug release**

In-vitro release behavior of trans-ferulic acid from TFA-NE was carried out through the dialysis bag (MW cut off 14000 Da). The *in-vitro* release profile of free trans-ferulic acid and TFA-NE in PBS pH 6.3 is shown in Fig. 3.13. The cumulative release amount of free trans-ferulic acid was found to be 30.71 % release in pH 6.3 at 14 hrs due to the low aqueous solubility. This indicates
that trans-ferulic acid belongs to the BCS II class drug and has low aqueous solubility (low dissolution).

The solubility of trans-ferulic acid is limited in the aqueous medium (6 µg/ml), so this is the reason only 30.71% is released in PBS pH 6.3 previously reported in the literature.

In comparison, within the same period, the cumulative release amount of trans-ferulic acid from TFA-NE was found to be 85.40 in PBS pH 6.3 within 14 hrs. However, the cumulative release of trans-ferulic acid from TFA-NE is higher than the free trans-ferulic acid. This suggested that NEs had enhanced solubility, permeability, and dissolution of trans-ferulic acid(74).

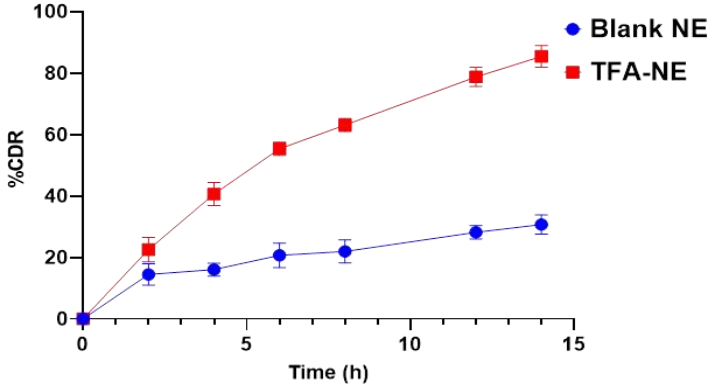

Figure 3.13. Representation *In-Vitro* drug released of free trans-ferulic acid and trans-ferulic acid loaded nanoemulsion

Released kinetics Models

Trans-ferulic acid loaded nanoemulsion optimized formulation was fitted into various release kinetic models, and the correlation coefficient (R2) value was found to be highest in the case of the zero order, i.e., 0.9986, as shown in tab.3.7, indicating that the trans-ferulic acid was released from the nanoemulsion follow a controlled released pattern.

Table 3.7: R^2 Values as per Different Release Kinetic Models.

Release Model	First order	Zero-order	Higuchi model	Hixon Crowell model	Korsmeyer-Peppas mode
R^2	0.7510	0.9986	0.9385	0.7594	0.8769

Stability studies of the nanoemulsion

Since nanoemulsions are thermodynamically unstable, they may separate or cream with time in storage. In order to speed up emulsion breakup, centrifugation was used as a stress condition to assess the stability of the freshly generated polymeric nanoemulsion. No signs of phase separation, creaming, or sedimentation were seen after centrifuging the sample for 30 minutes at 10,000 rpm in the case of NE and TFA-NE storage at 3±5^{0}C, but signs of these phenomena were seen after centrifuging the sample for 30 minutes at 10,000 rpm in the case of NE and TFA-NE storage at 40±2^{0}C/75±5% RH. Furthermore, NE and TFA-NE storage was maintained for three months in both rapid (40±2^{0}C/75±5%) and refrigerated conditions (3±5^{0}C) to verify long-term storage stability.

Every 30 days, samples were taken out and examined to see how the size distribution, polydispersity index, and zeta potential had changed. In contrast to samples held at 50°C, samples stored at 3±5^{0}C showed a substantial change in size, PDI, and zeta potential after three months, according to DLS data. For samples kept at 40±2^{0}C/75±5% temperature, no significant changes in size, PDI, or zeta potential were seen after three months. Since no significant changes in size (coalescence, aggregation) were noticed, the results, therefore, strongly imply that the nanoemulsion is more stable at refrigerator conditions (3±5^{0}C) for at least up to 3 months in terms of size change, PDI, and zeta potential.

Furthermore, nanoemulsions are unstable for at least three months at accelerated conditions (40±2^{0}C/75±5%) regarding size change, PDI, and zeta potential since significant changes were seen due to coalescence and aggregation. Examine if a nanoemulsion can stop the degradation of a loaded CLOT because there are no changes in drug entrapment that have been noticed. This

outcome made it abundantly evident that the nanoemulsion may shield the loaded medicine from degradation. The results indicate that nanoemulsions are less stable at accelerated conditions and more stable under cold conditions, as shown in Fig. 3.14(75).

Figure 3.14. Representation stability of the nanoemulsion at different conditions: A) size of B- NE, B) size of TFA-NE, C) PDI of B-NE, D) PDI of TFA-NE.

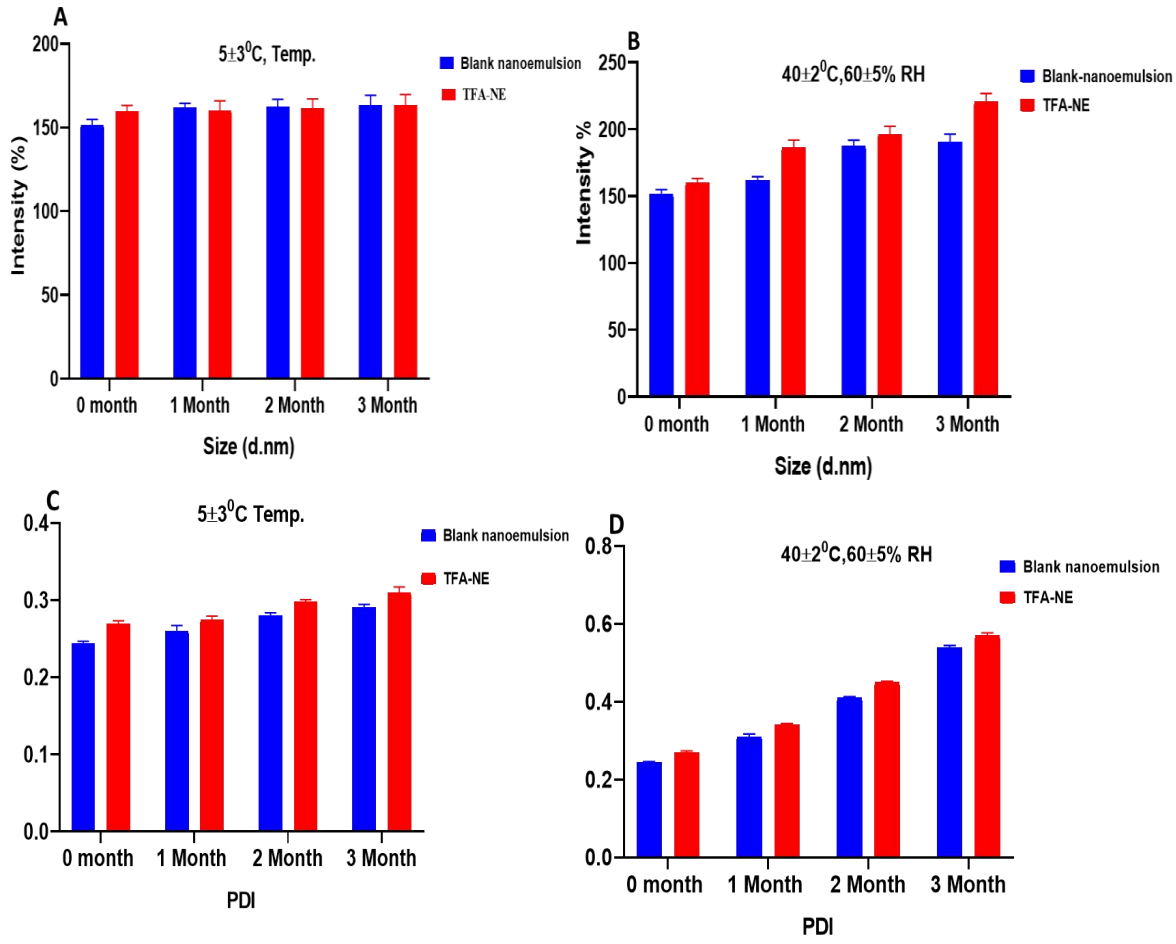

Anti-oxidant Activity by DPPH Radical Scavenging Assay

The antioxidant activity of trans-ferulic acid and TFA-NE is determined by DPPH assay. The mechanism changes the color from deep purple to pale yellow by reducing the DPPH free radical by hydrogen atom transfer. The DPPH radical forms stable molecules after being reduced by an antioxidant, and the activity of antioxidants can be evaluated by measuring these molecules at 517 nm. Trans-ferulic acid has the ability to scavenge free radicals. In the 125 µg/ml to 500 µg/ml concentration range, its scavenging effect was increased with dose, and the color of DPPH gradually became pale yellow with the increased concentration. In the present study, the scavenging ability of trans-ferulic acid and TFA-NE were found to be 65.03±0.07% and 71.21±0.1%, and the scavenging ability of TFA-NE on DPPH radical is higher than trans-ferulic acid as shown in fig 3.15. TFA-NE showed the potential to inhibit free radicals to produce a therapeutic effect(76).

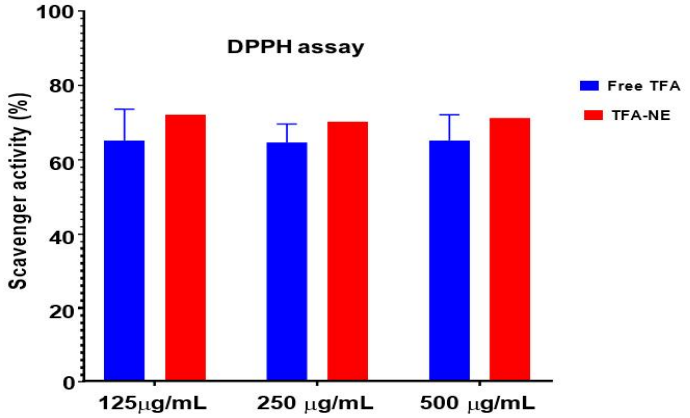

Figure 3.15. Percent (%) Scavenging Activities of Free Trans-Ferulic Acid and Trans-Ferulic Acid-Loaded Nanoemulsion by DPPH Assay.

Cell viability

The cytotoxicity of SH-SY5Y cells treated with free-TFA and different TFA-NE was determined by MTT assay **(Fig. 3.16).** Viable cells produce mitochondrial dehydrogenase, reducing MTT (Yellow color dye) to formazan crystals (Purple color). The SH-SY5Y cells treated with fre-TFA and TFA-NE showed more than 90% cell viability at concentrations ranging from 20 to 100 µg/mL compared to control. The positive control results showed less than 5% cell viability due to their cytotoxic effct, while the negative control showed 100% cell viability. The TFA-NE formulation is non-toxic and can treat Alzheimer's disease(77,78).

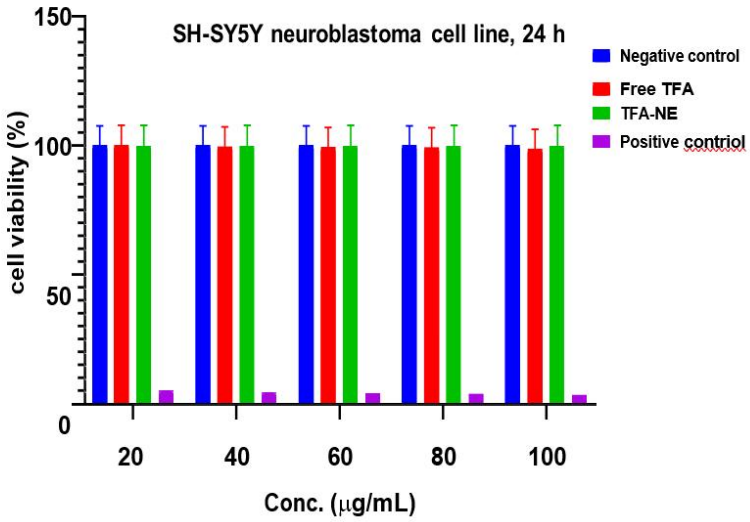

Figure 3.16. Cell viability (%) of SH-SY5Y cells after treatment with free-TFA and TFA-NE at different concentrations followed by 24-hour incubation was determined by MTT assay. Cell viability (%) was calculated concerning untreated cells (Negative control). Results were represented as mean ± SD (n = 3).

***In-vitro* AChE inhibitory activity**

The AChE inhibition ability of trans-ferulic acid was determined using Ellman's method. Ellman's method uses DTNB to quantify the thiocholine produced from the hydrolysis of acetylthiocholine by AChE. The AChE inhibition activity is determined by monitoring the yellow color formation resulting from the reaction between acetylthiocholine and DTNB in the presence of AChE. The results showed that free-TFA exhibited significant

AChE inhibitory activity of 35.48 ± 4.64 % at a concentration of 10 mM, suggesting that it may have potential as a therapeutic agent for AD. The TFA-NE formulation showed an AChE inhibition of 48.14±4.64 respectively (Fig.3.17). Through kinetic studies, it was found that the TFA-NE acts as a non-competitive inhibitor of AChE, indicating that the ME binds to a site on the enzyme distinct from the active site and alters its conformation. Although our findings suggest that TFA-NE has the potential as a therapeutic agent for treating AChE-related disorders, further studies are needed to evaluate their safety and efficacy in animal models(76,79).

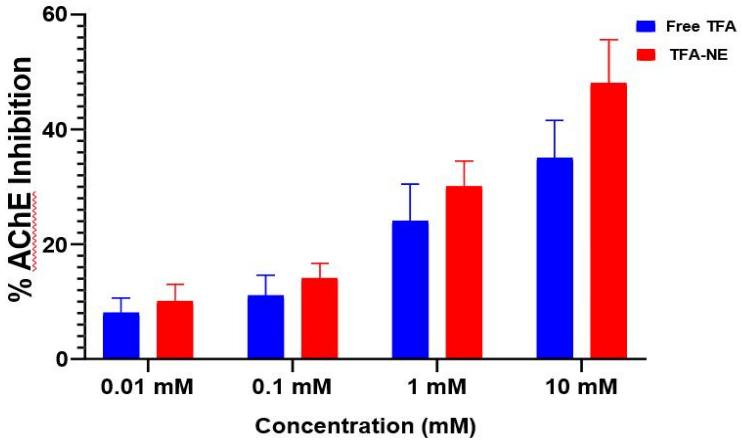

Figure 3.17. ***In-vitro*** **AChE inhibitory activity-free TFA and TFA-N**

Summary :

Trans-ferulic acid (TFA), a natural compound found in foods like barley, citrus, and rice, has anti-inflammatory and antioxidant properties. It inhibits β-amyloid peptides and promotes neuronal survival, making it a potential therapeutic for Alzheimer's disease (AD). However, its low oral bioavailability (9-20%) due to first-pass metabolism necessitates alternative delivery routes. This study employs a TFA-loaded nanoemulsion via the nasal route to enhance brain delivery, bypassing first-pass metabolism and ensuring rapid therapeutic action.

The nanoemulsion, formulated with lavender oil, Tween 20, and PEG 200, improves TFA's solubility and stability. Characterization via DLS, SEM, and TEM confirmed its optimal particle size and structure. FTIR and DSC studies demonstrated compatibility of excipients, while DPPH assays highlighted strong antioxidant activity. In-vitro diffusion studies showed enhanced solubility and bioavailability, supporting the nanoemulsion's potential for effective AD treatment.

Conclusion :

This research focuses on developing a trans-ferulic acid-loaded nanoemulsion (TFA-NE) for Alzheimer's disease (AD) treatment via nasal delivery, addressing TFA's low solubility and bioavailability (BCS Class II). The nanoemulsion enhances solubility, as shown by an in-vitro drug release study with cumulative release rates of 30.71%-85.40% over 14 hours at pH 6.3. TFA showed higher solubility in lavender oil (471.23 mg/mL), which also offers neuroprotective benefits. Tween 80 and PEG 200 were identified as optimal surfactant and co-surfactant, forming a stable o/w nanoemulsion with an average globule size of 125.9-152.6 nm and a zeta potential of -7.39 mV.

Characterization by FTIR, DSC, TEM, and DLS confirmed compatibility, stability, and spherical morphology. Samples remained stable under refrigerated conditions (3±5°C) for three months without significant changes in size or PDI. Antioxidant activity (DPPH scavenging) was higher for TFA-NE (71.21%) compared to free TFA (65.03%). SH-SY5Y cell viability exceeded 90% at concentrations of 20-100 µg/mL, and AChE inhibition was 48.14%, highlighting its therapeutic potential for AD.

REFERENCES :

1. Noori S, Zeynali F, Almasi H. Antimicrobial and antioxidant efficiency of nanoemulsion- based edible coating containing ginger (Zingiber officinale) essential oil and its effect on safety and quality attributes of chicken breast fillets. Food Control. 2018 Feb;84:312–20.
2. Kinney JW, Bemiller SM, Murtishaw AS, Leisgang AM, Salazar AM, Lamb BT. Inflammation as a central mechanism in Alzheimer's disease. Alzheimer's & Dementia: Translational Research & Clinical Interventions. 2018 Jan 5;4(1):575–90.
3. Ortiz N, Jiménez MF, Chaverri C, Cicció JF, Díaz C. Effect on cell growth, viability and migration of geraniol and geraniol-containing essential oil from *Lippia alba* (Verbenaceae) on gastric carcinoma cells. Journal of Essential Oil Research. 2022 Jan 2;34(1):65–76.
4. Caselli RJ, Reiman EM. Characterizing the Preclinical Stages of Alzheimer's Disease and the Prospect of Presymptomatic Intervention. Journal of Alzheimer's Disease. 2012 Dec 27;33(s1):S405–16.
5. Pavoni L, Perinelli DR, Bonacucina G, Cespi M, Palmieri GF. An Overview of Micro- and Nanoemulsions as Vehicles for Essential Oils: Formulation, Preparation and Stability. Nanomaterials. 2020 Jan 12;10(1):135.

6. Zhang XX, Tian Y, Wang ZT, Ma YH, Tan L, Yu JT. The Epidemiology of Alzheimer's Disease Modifiable Risk Factors and Prevention. J Prev Alzheimers Dis. 2021;1–9.
7. Pilong P, Chuesiang P, Mishra DK, Siripatrawan U. Characteristics and antimicrobial activity of microfluidized clove essential oil nanoemulsion optimized using response surface methodology. J Food Process Preserv. 2022 Dec 12;46(12).
8. Harwansh RK, Mukherjee PK, Bahadur S, Biswas R. Enhanced permeability of ferulic acid loaded nanoemulsion based gel through skin against UVA mediated oxidative stress. Life Sci. 2015 Nov;141:202–11.
9. Qian C, Decker EA, Xiao H, McClements DJ. Physical and chemical stability of β-carotene- enriched nanoemulsions: Influence of pH, ionic strength, temperature, and emulsifier type. Food Chem. 2012 Jun;132(3):1221–9.
10. Cascone S, Lamberti G. Hydrogel-based commercial products for biomedical applications: A review. Int J Pharm. 2020 Jan;573:118803.
11. Ahmed EM. Hydrogel: Preparation, characterization, and applications: A review. J Adv Res. 2015 Mar;6(2):105–21.
12. Kolaj I, Wang Y, Ye K, Meek A, Liyanage SI, Santos C, et al. Ferulic acid amide derivatives with varying inhibition of amyloid-β oligomerization and fibrillization. Bioorg Med Chem. 2021 Aug;43:116247.
13. Kadiya K, Ghosh S. Conversion of Viscous Oil-in-Water Nanoemulsions to Viscoelastic Gels upon Removal of Excess Ionic Emulsifier. Langmuir. 2019 Dec 31;35(52):17061–74.
14. Ozturk B, Argin S, Ozilgen M, McClements DJ. Nanoemulsion delivery systems for oil- soluble vitamins: Influence of carrier oil type on lipid digestion and vitamin D3 bioaccessibility. Food Chem. 2015 Nov;187:499–506.
15. Gué E, Since M, Ropars S, Herbinet R, Le Pluart L, Malzert-Fréon A. Evaluation of the versatile character of a nanoemulsion formulation. Int J Pharm. 2016 Feb;498(1–2):49–65.
16. Narayanasamy P, Switzer BL, Britigan BE. Prolonged-acting, multi-targeting gallium nanoparticles potently inhibit growth of both HIV and mycobacteria in co-infected human macrophages. Sci Rep. 2015;5.
17. Scotece M, Conde J, Abella V, Lopez V, Pino J, Lago F, et al. New drugs from ancient natural foods. Oleocanthal, the natural occurring spicy compound of olive oil: a brief history. Drug Discov Today. 2015 Apr;20(4):406–10.
18. Moghimi R, Ghaderi L, Rafati H, Aliahmadi A, McClements DJ. Superior antibacterial activity of nanoemulsion of Thymus daenensis essential oil against E. coli. Food Chem. 2016 Mar;194:410–5.
19. Choi S ryoung, Britigan BE, Narayanasamy P. Treatment of Virulent Mycobacterium tuberculosis and HIV Coinfected Macrophages with Gallium Nanoparticles Inhibits Pathogen Growth and Modulates Macrophage Cytokine Production. mSphere. 2019 Aug 28;4(4).
20. Li L, Chang H, Yong N, Li M, Hou Y, Rao W. Superior antibacterial activity of gallium based liquid metals due to Ga3+induced intracellular ROS generation. J Mater Chem B. 2021 Jan 7;9(1):85–93.
21. Singh Y, Meher JG, Raval K, Khan FA, Chaurasia M, Jain NK, et al. Nanoemulsion: Concepts, development and applications in drug delivery. Journal of Controlled Release. 2017 Apr;252:28–49.
22. Guglielmetti L, Mougari F, Lopes A, Raskine L, Cambau E. Human infections due to nontuberculous mycobacteria: the infectious diseases and clinical microbiology specialists' point of view. Future Microbiol. 2015 Sep;10(9):1467–83.
23. Kotta S, Khan AW, Ansari SH, Sharma RK, Ali J. Formulation of nanoemulsion: a comparison between phase inversion composition method and high-pressure homogenization method. Drug Deliv. 2015 May 19;22(4):455–66.
24. Mirsaeidi M, Vu A, Leitman P, Sharifi A, Wisliceny S, Leitman A, et al. A Patient-Based Analysis of the Geographic Distribution of Mycobacterium avium complex,
25. Mycobacterium abscessus , and Mycobacterium kansasii Infections in the United States. Chest. 2017 Apr;151(4):947–50.
Komaiko JS, McClements DJ. Formation of Food-Grade Nanoemulsions Using Low- Energy Preparation Methods: A Review of Available Methods. Compr Rev Food Sci Food Saf. 2016 Mar 8;15(2):331–52.
26. Jönsson BE, Gilljam M, Lindblad A, Ridell M, Wold AE, Welinder-Olsson C. Molecular Epidemiology of *Mycobacterium abscessus* , with Focus on Cystic Fibrosis. J Clin Microbiol. 2007 May;45(5):1497–504.
27. Azeem A, Rizwan M, Ahmad FJ, Iqbal Z, Khar RK, Aqil M, et al. Nanoemulsion Components Screening and Selection: a Technical Note. AAPS PharmSciTech. 2009 Mar 16;10(1):69–76.
28. Orme IM, Ordway DJ. Host Response to Nontuberculous Mycobacterial Infections of Current Clinical Importance. Infect Immun. 2014 Sep;82(9):3516–22.
29. Bandyopadhyay S, Beg S, Katare O, Sharma G, Singh B. QbD-Oriented Development of Self-Nanoemulsifying Drug Delivery Systems (SNEDDS) of Valsartan with Improved Biopharmaceutical Performance. Curr Drug Deliv. 2015 Nov 4;12(5):544–63.
30. Fang Z, Sampson SL, Warren RM, Gey van Pittius NC, Newton-Foot M. Iron acquisition strategies in mycobacteria. Tuberculosis. 2015 Mar;95(2):123–30.